2006

Atmospheric Radiation Measurements Aerosol Intensive Operating Period: Comparison of aerosol scattering during coordinated flights

Atmospheric Radiation Measurements Aerosol Intensive Operating Period: Comparison of aerosol scattering during coordinated flights

A. G. Hallar,[1,2] A. W. Strawa,[1] B. Schmid,[3] E. Andrews,[4] J. Ogren,[4] P. Sheridan,[4] R. Ferrare,[5] D. Covert,[6] R. Elleman,[6] H. Jonsson,[7] K. Bokarius,[1] and A. Luu[1]

Received 22 May 2005; revised 15 November 2005; accepted 20 January 2006; published 9 March 2006.

[1] In May 2003, a Twin Otter airplane, equipped with instruments for making in situ measurements of aerosol optical properties, was deployed during the Atmospheric Radiation Measurements (ARM) Program's Aerosol Intensive Operational Period in Oklahoma. Several of the Twin Otter flights were flown in formation with an instrumented light aircraft (Cessna 172XP) that makes routine in situ aerosol profile flights over the site. This paper presents comparisons of measured scattering coefficients at 467 nm, 530 nm, and 675 nm between identical commercial nephelometers aboard each aircraft. Overall, the agreement between the two nephelometers decreases with longer wavelength. During the majority of the flights, the Twin Otter flew with a diffuser inlet while the Cessna had a 1 μm impactor, allowing for an estimation of the fine mode fraction aloft. The fine mode fraction aloft was then compared to the results of a ground-based nephelometer. Comparisons are also provided in which both nephelometers operated with identical 1 μm impactors. These scattering coefficient comparisons are favorable at the longer wavelengths (i.e., 530 nm and 675 nm), yet differed by approximately 30% at 467 nm. Mie scattering calculations were performed using size distribution measurements, made during the level flight legs. Results are also presented from Cadenza, a new continuous wave cavity ring-down (CW-CRD) instrument, which compared favorably (i.e., agreed within 2%) with data from other instruments aboard the Twin Otter. With this paper, we highlight the significant implications of coarse mode (larger than 1 μm) aerosol aloft with respect to aerosol optical properties.

Citation: Hallar, A. G., et al. (2006), Atmospheric Radiation Measurements Aerosol Intensive Operating Period: Comparison of aerosol scattering during coordinated flights, *J. Geophys. Res.*, *111*, D05S09, doi:10.1029/2005JD006250.

1. Introduction

[2] Critical in the understanding of the Earth's radiation budget is the effect of aerosols, yet significant uncertainties in the radiative properties of aerosols globally and on regional scales prevent the needed accuracy within numerical models to define future climate change [*Houghton et al.*, 2001]. Thus the Intergovernmental Panel on Climate Change (IPCC 2001) has identified the radiative forcing of aerosols in urgent need of further research. Aerosols in the troposphere and stratosphere have both a direct and indirect effect on the radiation budget. Directly, aerosols can have either a cooling or warming effect on the Earth's surface depending on the composition of the particles and surface albedo. Some particles (such as dust and sulfate) mainly reflect and scatter incoming solar radiation, while others (such as soot) readily absorb it. Even when considering only the direct effect of aerosols on global climate, the uncertainty is estimated to be nearly the same magnitude as the effect (-0.4 ± 0.3 W/m^2) [*Hansen et al.*, 1998]. Furthermore, induced changes in regional radiative fluxes by aerosols can be an order of magnitude larger than the global mean forcing of greenhouse gases [*Krishnan and Ramanathan*, 2002].

[3] Because of the critical role of aerosols in climate prediction, in situ measurements of the optical properties of atmospheric aerosols have increased dramatically in the last two decades [e.g., *Anderson et al.*, 2003; *Clarke and Charlson*, 1985; *Clarke et al.*, 2001]. There have been several large airborne field campaigns to measure microphysical and optical properties of aerosol aloft. These field campaigns include the Aerosol Characterization Experiments (ACE), involving (among others) the National Center for Atmospheric Science (NCAR) C-130 and the Center for Interdisciplinary Remotely-Piloted Aircraft Studies (CIRPAS) Twin Otter and Pelican. The most recent was ACE-Asia, the fourth in this series of experiments organized

[1]NASA Ames Research Center, Moffett Field, California, USA.
[2]National Research Council Associateship Program, Washington, D. C., USA.
[3]Bay Area Environmental Research Institute, Sonoma, California, USA.
[4]NOAA, Climate Monitoring and Diagnostics Laboratory, Boulder, Colorado, USA.
[5]NASA Langley Research Center, Hampton, Virginia, USA.
[6]Department of Atmospheric Science, University of Washington, Seattle, Washington, USA.
[7]Center for Interdisciplinary Remotely-Piloted Aircraft Studies, Marina, California, USA.

0148-0227/06/2005JD006250

by the International Global Atmospheric Chemistry Program, which took place during the spring of 2001 off the coast of China, Japan and Korea [*Huebert et al.*, 2003].

[4] Measurements of aerosols aloft aboard aircraft, such as those in the ACE-Asia field campaign, typically require sampling from a external flow stream moving approximately 100 m/s [*Hegg et al.*, 2005]. Sampling supermicron particles within these airborne conditions is especially difficult, due in part to the rapid and large flow deceleration required to couple the exterior air stream into the aircraft instrumentation. [e.g., *Blomquist et al.*, 2001; *Huebert et al.*, 1990, 2004; *Murphy and Schein*, 1998; *Hermann et al.*, 2001; *Kramer and Afchine*, 2004]. Because of this sampling issue, there exists a measurement bias toward aerosols within the fine mode (approximately <1 μm); the presence (and thus optical properties) of coarse mode particles, i.e., supermicron particles, is often neglected in airborne aerosol measurements [*Collins et al.*, 2000]. This measurement bias is commonly accepted because of the assumption that aerosol radiative forcing is dominated by the fine particle mode.

[5] A recent study, using aerosol size distribution data from ACE 1 aboard the NCAR C-130 and the Pacific Exploratory Mission Tropics B (PEMT-B) aboard the NASA P-3B, was performed by *Shinozuka et al.* [2004]; this study investigated the uncertainty associated with airborne aerosol measurements due to aircraft inlet sampling performance. The *Shinozuka et al.* [2004] study used the transmission efficiencies from the Passing Efficiency of the Low Turbulence Inlet (PELTI) [*Huebert et al.*, 2004] experiments with data from the aforementioned campaigns. The calculated uncertainty due to particle losses within the inlet transmission dominated the total uncertainty in aerosol mass estimates. The uncertainty in scattering calculated from the optical particle counter distributions due to inlet transmission was +26%/−13%. Using a solid diffuser inlet in the recent DC-8 Inlet/Instrument Characterization Experiment (2003), demonstrated that inlet loss represented approximately 10% of the integral scattering values for both marine and dust environments (K. Moore, personal communication with Y. Shinozuka, 2003).

[6] Recognizing the difficultly of sampling supermicron particles from an airborne platform, the In situ Aerosol Profiles project (IAP) investigators elected to use a 1 μm impactor with the Cessna aircraft. *Andrews et al.* [2004] investigated the possibility of adjusting flight measurements on the basis of surface sampling. In that paper, measurements from the airborne nephelometer, operated with a 1 μm impactor, were compared with remote measurements of column aerosol optical depth. The surface-based nephelometer system, which alternates between two size cuts, a 1 μm and a 10 μm impactor, was used to estimate an upper limit of the amount of coarse aerosol present at altitude. The corrections, based on the assumption that the ratio of submicron to total extinction measured at the surface held for all nine levels of the aircraft profile, were applied to the Cessna nephelometer data. This assumption increased the total aerosol optical depth calculated with the Cessna nephelometer data by approximately 11%. This assumption improved comparisons between remote measurements (i.e., ground-based radiation instrumentation at ACRF and the Cessna nephelometer).

[7] Overall, the median value of scattering coefficients aloft appeared to be consistent (within 50%) with the surface measurements up to 1525 m and less consistent (within orders of magnitude) above that altitude [*Andrews et al.*, 2004]. Until vertical mixing occurs, the surface parameters will be decoupled from the parameters aloft [*Delle Monache et al.*, 2004]. Thus it is not expected that the surface nephelometer measurements will represent values aloft [*Andrews et al.*, 2004]. Because of the extreme variability in aerosol optical properties found at different altitudes, the surface nephelometer is not being used to correct the airborne nephelometer in the IAP data in this paper.

[8] With this paper, we explore the optical effects of coarse mode particles at altitude by taking advantage of the unique opportunity presented by Aerosol IOP. Aerosol IOP provided two different aerosol inlets measuring simultaneously with coordinated flights, allowing for estimations of the effect of inlet sampling conditions at altitude. Additionally, these coordinated flights facilitated comparisons of measured and derived aerosol optical properties [see *Andrews et al.*, 2006; *Strawa et al.*, 2006; *Ferrare et al.*, 2006]. We will present comparisons between commonly used measurement techniques (i.e., TSI nephelometers) and new, advanced instrumentation (i.e., Cadenza). Additionally, this paper will address the effects of sampling methods (i.e., the inlet cutoff diameter size) on in situ measurements of aerosol optical properties with theoretical results.

[9] Although a loss of large particles is unavoidable in the measurement of aerosols from an aircraft because of the aerodynamic limitations of inlets, this paper focuses on the need to investigate these losses (or active removal in the case of an impactor) and the resulting effects on the final data product. As stressed by *Wang et al.* [2002], the continued development of aerosol instruments, and thus sampling techniques, capable of accurately characterizing the size and shape of large particles will improve the ability to perform radiative closure of the effects of atmospheric aerosol.

2. Experiment

[10] In May 2003, an intensive flight mission was conducted as part of the Aerosol Intensive Operating Period (IOP) over the ARM Southern Great Plains Site in north central Oklahoma (36.74°N, 97.09°W, 319 m above sea level). Between 6 and 29 May, the CIRPAS (Center for Interdisciplinary Remotely-Piloted Aircraft Studies, based in Marina, California) Twin Otter unpressurized aircraft [e.g., *Bane et al.*, 2004] performed 16 research flights out of Ponca City, Oklahoma. For the Aerosol IOP campaign the maximum flight altitude was 5.6 km [*Schmid et al.*, 2006].

[11] Additionally, measurements were conducted with a light aircraft (the ARM Cessna 172XP) over the SGP site during the Aerosol IOP. This aircraft utilized a similar aerosol instrument package as found both on the Twin Otter and one located at the SGP ground site [*Sheridan et al.*, 2001; *Andrews et al.*, 2004]. This aircraft has a long history of measurements beginning in March 2000 over the SGP site in a project titled "In situ Aerosol Profiles at SGP" (IAP). The aircraft typically flies several times per week.

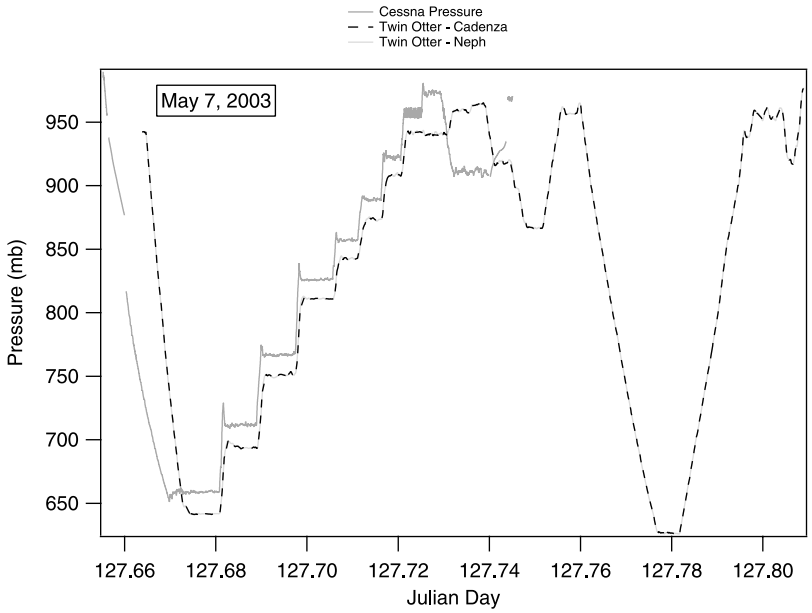

Figure 1. Illustration of the formation flight of the IAP Cessna and CIRPAS Twin Otter on 7 May 2003. The flight legs were flown in a "stair step" pattern between approximately 650 and 950 mb, corresponding to a range in altitude of approximately 2000–12,000 ft (60–360 m). The Cessna nephelometer pressure is measured downstream of the 1 μm impactor, and there is a pressure drop caused by the impactor (approximately 10 mb). This pressure drop in the Cessna causes the difference in the two aircraft instrumentation pressure measurements.

The flight times and days of the week are randomized, but the flights are limited to daylight hours. This project is a joint effort between the ARM program and the Climate Monitoring and Diagnostics Laboratory (CMDL) of the National Oceanic and Atmospheric Administration (NOAA). The objective of the IAP project is to obtain a statistically significant data set of the vertical distribution of aerosol properties above SGP [e.g., *Andrews et al.*, 2004].

[12] During the Aerosol IOP coordinated flights of the CIRPAS Twin Otter and the IAP Cessna aircraft were obtained, allowing for several simultaneous in situ data sets available for comparison. Five coordinated flights were accomplished on 7, 9, 17, 25, and 29 May 2003. Typically for each flight day, the Cessna flew nine level legs over or near the SGP site. These legs were flown at altitudes of 1500, 2000, 3000, 4000, 5000, 6000, 8000, 10,000, and 12,000 ft above sea level [*Andrews et al.*, 2004]. The two aircraft could not fly coordinated at the lowest-level leg altitude because of safety concerns. Two dates, 7 and 9 May, contained the maximum (eight) possible flight legs. Seven level legs were conducted on 25 May. Four level legs were flown on 17 May and two legs were flown on 29 May. Figure 1 illustrates level pressure legs flown by the Twin Otter and Cessna during Aerosol IOP on 7 May in a "stair-step" manner.

[13] One objective of the Aerosol IOP was to assess the accuracy of aerosol optical property (scattering, absorption, and extinction) measurements using a number of different instruments and techniques. This paper will examine comparisons of aerosol scattering measurements during time periods in which the Cessna and the Twin Otter aircraft flew in formation. Observations from several instruments are discussed in this paper including three wavelength integrating nephelometers, Cadenza and two particle sizing probes (PCASP and CAPS). A brief description of each instrument is given below.

2.1. CMDL: TSI 3563 Nephelometer

[14] The aerosol instrumentation payload inside the Cessna aircraft consists primarily of a TSI (Model 3563, St. Paul, Minnesota) integrating nephelometer and a Radiance Research particle soot absorption photometer (PSAP). The nephelometer measures total (7°–170°) and backward (90°–170°) light scattering by aerosol particles at three wavelengths: blue (450 nm), green (550 nm) and red (700 nm) [*Anderson et al.*, 1996; *Anderson and Ogren*, 1998]. The nephelometer was calibrated with particle-free air and CO_2 prior to and after the IOP and was zeroed with particle-free air twice during each flight.

[15] All nephelometer data were corrected for truncation and illumination based on the Ångström exponent as suggested by *Anderson and Ogren* [1998]. The nephelometer operated at a volumetric flow rate of approximately 27 L/min. Data were collected at 1-s sample rate. Auxiliary equipment includes a 1 micron impactor, corresponding to a geometric size cut of approximately 0.79 μm for particles of a density 1.6 g/cm^3, to exclude supermicron particles and a heater to ensure the relative humidity of the airstream is less than 40% RH. This impactor was used to limit two sources of uncertainty caused by supermicron aerosols: (1) uncertainty in the amount of inlet losses of large particles and (2) uncertainty in the truncation correction for supermicron particle sizes [*Andrews et al.*, 2004].

[16] *Anderson et al.* [1996] tested the TSI 3536 nephelometer using monodisperse commercial particles to investigate the uncertainty within the measurement of total

scattering for three wavelengths. The scattering coefficient was predicted for the commercial particles using Mie theory. The goal of this closure experiment was to validate that the average discrepancies between the actual nephelometer measurement and the independently predicted measurement were within the experimental uncertainties. Overall, errors arising from nephelometer nonidealities are less than 10% for submicron particles. Specifically the average general uncertainty in the TSI 3536 nephelometer for total scatter at the blue, green, and red wavelengths is 7.3%, 7.6%, and 9.8%. These reported uncertainties for the TSI 3536 nephelometer are represented in all succeeding figures. For coarse mode particles (diameter greater than 1 μm) nephelometer errors increase dramatically for total scattering (20–50%). This error increase is an effect of the inability of a nephelometer to sense near forward scattering, which is an increasing dominant part of total scattering for large particles [*Anderson et al.*, 1996].

2.2. University of Washington TSI 3563 Nephelometer

[17] The University of Washington participated in the Aerosol IOP mission with an integrating nephelometer and a three-wavelength PSAP absorption photometer located on the Twin Otter. This nephelometer was the same model as used aboard the Cessna, TSI Model 3563. The flow rate through the TSI was approximately 30 L/min with the inlet heater operational. The Twin Otter nephelometer data were also corrected for truncation and illumination based on the Ångström exponent as suggested by *Anderson and Ogren* [1998]. All uncertainty estimations with regard to the nephelometer discussed in the previous section apply to this instrument as well. Again the TSI 3563 nephelometer measures light scattering at three wavelengths (450 nm, 550 nm, and 700 nm), yet the scattering data were reported at slightly different wavelengths (467 nm, 530 nm, and 660 nm). The change in reported wavelength was performed for comparison with the three-wavelength PSAP. This nephelometer was calibrated against particle free air and CO_2 prior to the field deployment and zeroed with particle-free air before each flight. The scattering coefficients were reported at 8-s intervals, which roughly represent the sampling time of the TSI nephelometer. This time interval is determined by the instrument volume, flow rate, and electronic averaging time.

2.3. Cadenza

[18] Cadenza, a new aerosol optical instrument using cavity ring down (CRD) technique and a reciprocal nephelometry technique, participated in Aerosol IOP for the measurement of extinction and scattering at 675 nm and extinction at 1550 nm. First demonstrated by *O'Keefe and Deacon* [1988], the CRD technique has been used primarily for gaseous absorption spectroscopy (various papers in the work by *Busch and Busch* [1999]). The use of CRD to measure aerosol extinction is relatively new [e.g., *Smith and Atkinson*, 2001; *Strawa et al.*, 2003].

[19] In continuous wave CRD (which is used in Cadenza for the measurement of aerosol extinction) the laser is in resonance with the ring-down cell allowing laser power build up in the cell [*Romanini et al.*, 1997]. Energy build up within the cell makes it possible to also detect the aerosol scattering signal in Cadenza. Cadenza has a maximum theoretical circulating power of about 50 W; this estimate does not account for other losses within the cell. Additionally, the laser is turned off prior to power maximum, which allows the cell to ring-down. Operationally, an energy density of about 2 W/cm^2 within the cell is typical. These energy densities are not high enough to affect sample conditions [*Strawa et al.*, 2006].

[20] For Cadenza, the scattering signal is collected with two diffusers set into the cell wall above the point where the optical beams cross. The diffusers (Gamma Scientific Model 700-8D) have a Lambertian response from 5° to 175°. The diffuser for the 675 nm channel is connected to a photomultiplier tube (Hamamatsu Model R1464) with a light pipe. The diffuser for the 1550 nm channel is connected to an avalanche photodiode with a fiber optic cable.

[21] In a typical nephelometer design, such as the TSI 3563 nephelometer, the light source is transmitted through a diffuser or lens and the detector senses along an optical path [e.g., *Anderson et al.*, 1996]. With Cadenza, the optical arrangement is based on the reciprocal nephelometer design of *Mulholland and Bryner* [1994], wherein the illumination is provided by a laser along an optical path. The detector is then mounted orthogonal to the optical and flow axes to collect the light. There are several advantages to this approach. First, it is possible to obtain significantly better Lambertian diffusers than those commonly used with disperse light sources. Additionally, corrections for the spectral characteristics (of either the detector/filter assemble or the light source) are not required. Uncertainties due to the dependence of the scattering on the wavelength of light will depend on the effective line width of the instrument. Cadenza uses a laser of very narrow line width, compared to diffuse lamps used in traditional nephelometers. One further advantage of Cadenza is that measurements of extinction and scattering coefficients are made simultaneously with lab generated, nonabsorbing spheres. These measurements are then compared to remove effects due to angular nonidealities in the scattering measurement (see *Strawa et al.* [2006] for more details).

[22] Cadenza was able to measure scattering coefficient of 1 Mm^{-1} at 675 nm wavelength with an uncertainty of 10%. Instrument sensitivity is 0.3 Mm^{-1} for a 8 s average. The uncertainty in scattering coefficient is similar to the uncertainty recorded for TSI Model 3563 nephelometers for particles less than 1 μm in diameter [*Anderson et al.*, 1996; *Anderson and Ogren*, 1998]. The source of this absolute uncertainty is derived from an inability to measure the entire forward scattering lobe of an aerosol sample, [*Anderson and Ogren*, 1998] a problem that our reciprocal nephelometer design does share with the TSI nephelometer. Cadenza is corrected for this error using the same method as the TSI nephelometer: From our calibrations with commercial particles of different sizes (500 nm, 700 nm, and 900 nm), a correction factor is obtained as a function of Ångström exponent (derived from the 675 nm and 1550 nm extinction values). Mie calculations are used to obtain the "theoretical" correction factors. In data reduction procedure, we obtain the Ångström exponent and use the appropriate factor to correct for truncation error (see *Strawa et al.* [2006] for more details).

[23] Cadenza is the first airborne CRD instrument able to measure aerosol optical properties. The prototype Cadenza

instrument as described by *Strawa et al.* [2003] participated successfully in the Reno Aerosol Optics Study (RAOS) [*Sheridan et al.*, 2005]. Cadenza then flew its first and second successful airborne missions, Asian Dust Above Monterey (ADAM, April 2003) and Aerosol IOP, aboard the CIRPAS Twin Otter. Detailed descriptions of the instrument, the data analysis and comparisons with other methods during the entire Aerosol IOP are reported by *Strawa et al.* [2006]. Cadenza operated successfully on all 16 Aerosol IOP science flights continuously measuring σ_{ep} and σ_{sp} at 675 nm and 1550 nm. This paper will concentrate on the comparison of the scattering measurement results of Cadenza at 675 nm with those from the TSI nephelometer.

2.4. PCASP

[24] CIRPAS/Naval Postgraduate School operated a Passive Cavity Aerosol Spectrometer Probe (PCASP) aboard the Twin Otter during Aerosol IOP. The PCASP Model 100-X was developed by Particle Measuring Systems (PMS Inc., Boulder, Colorado) to measure aerosol particle size distributions. The PCASP, part of a general class of instruments called optical particle counters (OPCs), detect single particles and size them by measuring the intensity of light that the particle scatters when passing through a light beam. A Helium-Neon laser beam is focused to a small diameter at the center of an aerodynamically focused, particle laden air stream. Particles that encounter this beam scatter light in all directions and some of this light is collected by a mirror over angles from about 35° to 135°. This collected light is focused onto a photodetector and then amplified, conditioned, digitized and classified into one of twenty size channels. The size of the particle is determined by measuring the light scattering intensity and using Mie scattering theory to relate this intensity to the particle size [*Jonsson et al.*, 1995].

[25] During Aerosol IOP, the PCASP measured particles over a size range of 0.1–3.1 μm. The PCASP was wing mounted and measures at a low relative humidity (i.e., dry particles). There was not a relative humidity (RH) sensor within the PCASP, although the deicing heaters were on throughout the entire mission. Several years ago, a 20°C temperature increase created by these heaters was measured within the PCASP. The RH within the PCASP should be approximately zero (H. Jonsson, personal communication, 2005). Thus we assume that the relative humidity differences between the nephelometers (also operating ''dry'' with RH <30%) and the PCASP are negligible. The estimated uncertainty of the PCASP is ±20% for sizing and ±16% for concentration measurements. The PCASP is calibrated using monodispersed polystyrene latex beads [*Jonsson et al.*, 1995]. The size determined by the PCASP must be viewed with some caution when sampling mixed composition aerosol because the sizing method assumes that the scattered light is detected from a spherical particle with a refractive index of 1.58 (i.e., the polystyrene latex beads used in the calibration) and because particles dry out because of heating in the inlet [*Jonsson et al.*, 1995; *McFarquhar and Heymsfield*, 2001].

2.5. CAPS

[26] The Cloud, Aerosol, and Precipitation Spectrometer system (CAPS, Droplet Measurement Technology, Inc., Boulder, Colorado) contains CAS, a cloud and aerosol spectrometer and CIP (Cloud Imaging Probe), which is an occultation system that measures the size of precipitation particles. The CAS system measures both forward and backward scatter from particles and independently bins the measured pulse heights into a selectable number of bins.

[27] During Aerosol IOP, the CAPS measured particles over a size range of: 0.63–63.3 μm. The CAPS was also wing mounted and measured at ambient conditions. The estimated uncertainty in the accuracy the CAPS is ±20% for sizing and ±16% for concentration measurements [*Baumgardner et al.*, 2001].

2.6. Inlet Systems

[28] The Cessna aerosol inlet nozzle is an aerodynamic diffuser design with slightly rounded edges and an internal diffuser angle of 6.5°. The inlet was designed to be isokinetic at the typical aircraft sampling airspeed (50 m/s) and sample flow rate (30 L/min). As mentioned in the above sections (2.1 and 2.2), the Cessna IAP aircraft is equipped with a 1 μm impactor that removes aerosols with an aerodynamic diameter greater than 1 μm, which is equivalent to a 0.79 μm geometric diameter assuming a particle density of 1.6 g cm^{-3}.

[29] The Twin Otter was equipped with one community aerosol inlet, from which Cadenza, the nephelometer, and several other instruments received their sample intake. This community inlet consists of a two-stage diffuser. The inlet sampled from a shrouded intake whose nominal 50% cutoff diameter was determined to be 8 μm. These characteristics of the inlet were determined by a flight test comparison of cross-calibrated interior and exterior Forward Scattering Spectrometer Probe (FSSP) Model 100x optical probes in 2001 prior to ACE-Asia field campaign [*Gao et al.*, 2003]. The probes were calibrated using National Institute of Standards and Technology (NIST) traceable uniform polystyrene spheres. The inlet was not modified since the ACE-Asia campaign. Most recently, *Hegg et al.* [2005] has also quantitatively assessed the transmission efficiency of the CIRPAS Twin Otter inlet as a function of particle size. Using the same methodology as in the past [*Gao et al.*, 2003], the inlet transmission efficiency was again measured with a comparison of interior and exterior particle size distributions in flight using FSSP-100x probes [*Hegg et al.*, 2005]. Additionally, the inlet was tested in the Kirsten Wind Tunnel at the University of Washington using two 90° scattering white light optical particle counters (Welas Model 1200) with a free stream reference measurement. Overall, the recent results of *Hegg et al.* [2005] are similar to the inlet test in 2001 [*Gao et al.*, 2003]. *Hegg et al.* [2005] found a transmission efficiency of 60% at sizes between 5.5 μm and the limit of their test measurements, 9 μm. This inlet system thus allowed for the sampling of larger particles on the Twin Otter aircraft than sampled on the Cessna IAP aircraft.

[30] No impactor was typically used with the nephelometer aboard the Twin Otter, except for the first 2 hours of 25 May when a 1 μm impactor was attached. This time period corresponded to the flight legs flown in coordination with the Cessna IAP aircraft on 25 May. This impactor was not attached to the community inlet, but separately attached to the intake for only the nephelometer and the PSAP

Table 1. Flight Dates and Time Periods of Simultaneous Level Leg Comparisons Between Instruments Aboard the IAP Cessna Aircraft and the CIRPAS Twin Otter[a]

Number	Date, yyyymmdd	Start Time, Fractional Julian Day	End Time, Fractional Julian Day	Pressure Twin Otter, mb	Ave. 675 nm Scattering Twin Otter Neph, Mm^{-1}	Standard Deviation in Scattering. Mm^{-1}	Standard Deviation in Scattering, %
1	20030507	127.67419	127.68103	642	18.7	1.28	6.83
2	20030507	127.68389	127.68812	694	8.6	0.79	9.22
3	20030507	127.69101	127.69636	750	7.2	0.81	11.3
4	20030507	127.70026	127.70583	811	6.3	0.73	11.6
5	20030507	127.70651	127.71085	841	5.9	0.67	11.4
6	20030507	127.71278	127.71647	874	7.4	1.39	18.8
7	20030507	127.72161	127.72519	941	7.1	0.77	10.8
8	20030507	127.73177	127.73598	959	6.8	0.42	6.2
9	20030509	129.77581	129.78118	636	29.1	9.10	31.2
10	20030509	129.78432	129.79018	687	33.6	4.29	12.8
11	20030509	129.79566	129.79957	742	36.1	5.18	14.3
12	20030509	129.80106	129.80529	803	19.3	0.74	3.9
13	20030509	129.82484	129.82893	934	32.1	3.10	9.7
14	20030517	137.85362	137.85868	814	14.1	1.19	8.4
15	20030525	145.80100	145.80528	645	32.6	18.80	57.6
16	20030525	145.80809	145.81383	698	15.0	9.76	64.9
17	20030525	145.82636	145.83289	815	2.5	0.72	29.1
18	20030525	145.83568	145.83951	879	20.3	1.32	6.5
19	20030525	145.84079	145.84387	913	19.3	0.91	4.7
20	20030525	145.84516	145.84803	947	17.4	0.76	4.3

[a]Additional information, including the average scattering coefficient of Twin Otter nephelometer at 675 nm along with the calculated standard deviation from this average value, is provided to demonstrate the variability of the scattering coefficients during flight legs.

absorption instrument. When the impactor was in place, a comparison could be made between the Twin Otter and Cessna nephelometers, both with a 1 μm impactor in the sample line.

3. Case Studies

[31] Case studies were carefully chosen using the following requirements, after all instrument clocks were adjusted to reflect a common Universal Time (Twin Otter Cabin Time). In order to have accurate time stamps the Payload Data Management System time aboard the Twin Otter was synchronized with GPS time. A GPS receiver was used as the time standard on the Cessna. Times are reported in all figures as fractional Julian Days.

[32] 1. Level legs were only considered if the duration of the leg was four minutes or greater.

[33] 2. During each "level" leg the ambient pressure of the Cessna aircraft and Twin Otter aircraft did not fluctuate greatly. Level legs were only considered if the pressure change during the level leg was less than ±3 mb for both aircraft.

[34] 3. All instruments fundamental to this comparison were operating.

[35] The date, time period, and ambient pressure of all "level" legs are listed in Table 1. In general, in most of level flight legs the scattering coefficient remained relatively constant. Out of the 20 level flight legs, only four had a standard deviation from the average scattering value greater than 20% (when considering the data from the Twin Otter nephelometer red scattering channel). These four deviant legs include legs 9, 15, 16, and 17. Leg 17 represents low values of scattering (~2 Mm^{-1}), and thus the high standard deviations may simply represent limits in measurement capability. During the level flight legs 9 and 16, it appears that both aircraft encountered aerosol with a constant higher values (approximately 40 Mm^{-1}) of scattering coefficients during several minutes of flight. Finally, during leg 15 both aircraft entered several plumes, with values of scattering coefficient as high as 80 Mm^{-1} at 675 nm. The average scattering coefficient and standard deviation are presented in Table 1.

3.1. Comparison Conditions

[36] In order to facilitate a proper comparison, all instruments should be compared at the same wavelengths. Thus Ångström wavelength corrections were made [*Ångström*, 1929] in this study. The Ångström exponent was derived from each of the TSI nephelometers and used to correct the instruments' wavelengths respectively. The instruments are compared at the following wavelengths for the red, green and blue channels: 675 nm, 530 nm, and 467 nm to match the PSAP wavelengths.

[37] Additionally, all instruments were compared at standard temperature and pressure (STP, i.e., 1013 mb and 273.15 K). These instruments were all operated "dry." In this paper, dry is defined as a relative humidity (RH) less than 30%. This assumption is supported by the work of *Tang and Munkelwitz* [1994], which states that at 30% RH most of the hygroscopic aerosols are dehydrated except for a few highly hygroscopic salts such as NH_4HSO_4 and $NaHSO_4$. The maximum difference between the RH of all instruments was less than 10%. Figure 2 illustrates the RH measured separately by Cadenza and the TSI nephelometer aboard the Twin Otter, and the RH measured aboard the IAP Cessna on 7 May.

[38] Given the close proximity (approximately 500 feet) of the two aircraft during these level leg comparisons, along with the similar RH measured aboard each aircraft, we will here after assume that the two planes flew within the same aerosol sample. This is a reasonable assumption for the level flight legs averaging between 4 and 10 min

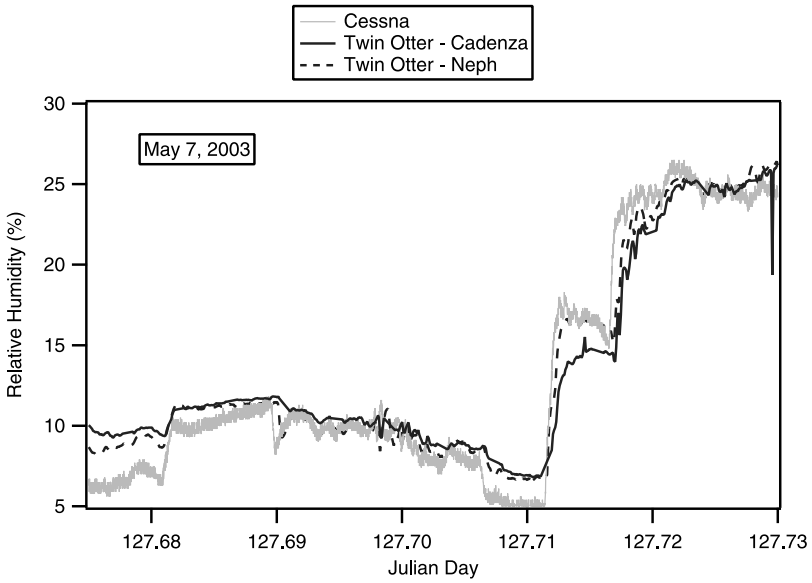

Figure 2. Relative humidity (RH) measured within the nephelometer aboard the Cessna IAP and the nephelometer and Cadenza aboard the Twin Otter. Only the time corresponding to the coordinated flight legs between the Twin Otter and the Cessna on 7 May is illustrated. All measurements were sampled "dry," or with a RH below 30%. This decrease in RH from ambient RH (not shown), caused by an increase in temperature, was partially due to ram heating within the inlet and partially due to heating of the sample line as it carried aerosol from the inlet to the instrument. In the case of the nephelometers, the light source also heats the aerosol sampled.

in duration; we are not making this assumption for instantaneous comparisons.

3.2. Aerosol Composition

[39] The U.S. Department of Energy established the ACRF site in Oklahoma in 1992 as the first of its field measurement sites [*Stokes and Schwartz*, 1994]. This site has provided one of the longest continuous records of aerosol measurements. *Sheridan et al.* [2001] conducted a study of the initial 4-year record of surface measurements from the ACRF site. In general, the atmospheric aerosols over the site were described as mixed regional aerosols, although some large point source emissions, notably oil refineries and power plants, may influence the site occasionally. Additional local aerosol sources (e.g., field burning episodes and vehicular traffic) sporadically affect the surface measurements [*Sheridan et al.*, 2001]. The aerosols over the site were generally hygroscopic with a 4 year median f(RH) value of 1.83. Smoke and dust influence made the aerosols less hygroscopic and lowered the ambient f(RH) median values of 1.55 and 1.59 respectively [*Sheridan et al.*, 2001].

[40] Aerosol mass and composition were measured as a function of size (8 modes, 6 submicron) and time (continuous, 3 hour analyses), at the ACRF ground site during AIOP by Tom Cahill and the UC Davis DELTA Group. Local effects were minor, but the site exhibited changing impacts from regional (Houston, Texas, 13 May), national (Ohio Valley sulfates, 17 May), international (agricultural burning in Central America, 7 and 8 May), and intercontinental (African dust, 7 and 8 May) sources that in some cases represented the highest concentration of aerosols seen in the period (T. Cahill, personal communication, 2005).

[41] Aerosol ionic components, including ammonium, sulfate, nitrate, potassium, calcium, magnesium, sodium, chloride, oxalate, formate, and acetate, were measured on the ground using a particle-into-liquid sampler coupled to ion chromatography technique, for particles smaller than 1 μm in diameter, during the daytime for Aerosol IOP at the ACRF site. The results showed that ammonium and sulfate were the dominant ions with a typical molar ratio close to 2 to1 [*Lee et al.*, 2003].

[42] *Ferrare et al.* [2006] describe aerosol at ACRF AIOP as relatively nonabsorbing boundary layer aerosols. Yet on 25–28 May, satellite imagery and back trajectory analyses indicate that elevated, relatively nonabsorbing aerosol layers located between 2.6 and 3.6 km were smoke layers produced by Siberian forest fires [*Damoah et al.*, 2004; *Jaffe et al.*, 2004; P. R. Colarco et al., Elevated injection height, long-range transport, and evolution of a Siberian forest fire smoke plume, manuscript in preparation, 2005]. Smoke from Siberian forest fires, which passed over the site at altitude was not seen in ground-based samples measured by the DELTA Group (T. Cahill, personal communication, 2005).

4. Results

4.1. Comparison of Scattering Aboard the Twin Otter: Cadenza and Nephelometer

[43] During all the case studies described in section 3 in which the Twin Otter nephelometer was not connected to an impactor, the red (675 nm) scattering coefficients measured aboard the Twin Otter using Cadenza and the TSI nephelometer compared extremely well. During these level legs both Cadenza and the nephelometer measured from the

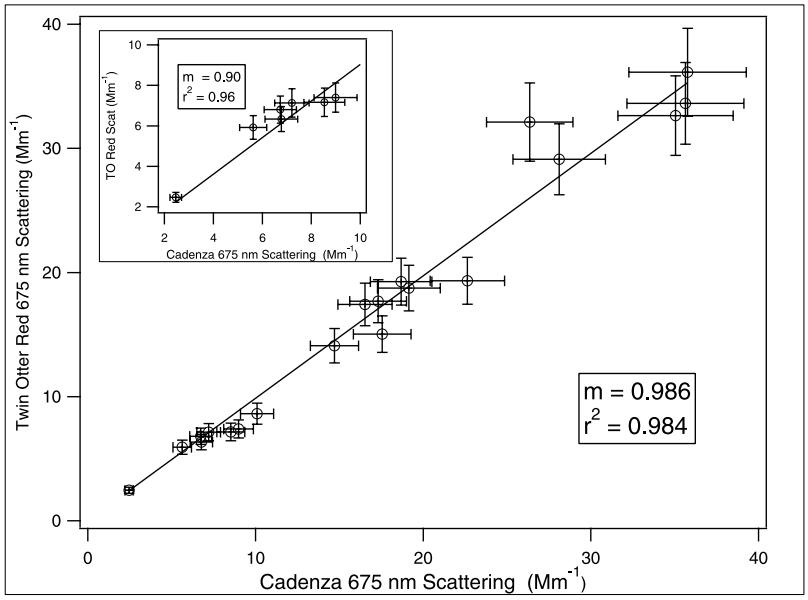

Figure 3. Excellent agreement in average scattering coefficient at 675 nm seen during all flight legs between Cadenza and the TSI nephelometer aboard the CIRPAS Twin Otter. Error bars represent the 9.8% uncertainty [*Anderson et al.*, 1996] in the measurement of the TSI nephelometer and the 10% uncertainty of Cadenza. An extensive discussion of comparisons between these two instruments during the entire Aerosol IOP campaign is given by *Strawa et al.* [2006].

same community inlet. Figure 3 illustrates this comparison for the average scattering coefficients during each level leg measured by both instruments. During all legs, the instruments agreed within 2% (slope = 0.986) with a good correlation of $r^2 = 0.984$ (Note: the linear curve fitting has a forced zero y-intercept). For only low values of scattering (shown in Figure 3, top left corner), i.e., less than 10 Mm^{-1}, the comparison is not quite as robust. Yet, the instruments still agreed within 10% (slope = 0.90), again with a good correlation of 0.96. Overall, this is a strong confirmation of the accuracy of these instruments. These two very different techniques provided a robust agreement and correlation. A more extensive comparison of Cadenza with the TSI nephelometer is provided by *Strawa et al.* [2006].

4.2. In-Flight Comparison Between Cessna and Twin Otter Nephelometers

[44] First, both the TSI nephelometers, one aboard the Cessna IAP aircraft and the other aboard the Twin Otter aircraft, were compared for all flight legs, except those on 25 May during which the Twin Otter nephelometer was attached to a 1 μm impactor. This large subset of flight legs represents typical flight conditions both for the Cessna IAP aircraft (i.e., equipped with a 1 μm impactor) and the CIRPAS Twin Otter aircraft (inlet with a 50% cutoff diameter at approximately 8 μm). Figure 4 illustrates the comparison between the nephelometers for all three wavelengths. Data are averaged over the duration of each flight leg for the comparison. This comparison includes data from 14 level flight legs. The agreement was best at the shortest wavelength (blue 467 nm), with a slope 0.928 between the two instruments (Note: all linear curve fitting have a forced zero y-intercept). The comparison was not as good at the longer wavelengths. As shown in Figure 4, the comparison at 530 nm gives a slope of 0.681 and at 675 nm a slope of 0.610 was obtained. These two instruments were well correlated with an r-squared value of 0.95 or greater. These numbers are highlighted in Table 2. Overall, Figure 4 illustrates that the agreement between the two nephelometers decreases with longer wavelength. This behavior suggests that the Cessna IAP nephelometer is not measuring larger particles present in the sample (i.e., the Cessna inlet system actively removed these aerosol present in the atmosphere), which scatter more effectively at longer wavelengths.

[45] A commonly reported intensive aerosol property is the fine mode fraction of light scattering (FMF_{scat}). FMF_{scat} is related to the fine mode-to-total aerosol mass ratio, which can be readily calculated in chemical transport models. Typically, the FMF_{scat} is calculated by taking a ratio of scattering measured with a nephelometer attached to a 10 μm impactor and submicron light scattering measured with a nephelometer attached to a 1 μm [*Doherty et al.*, 2005]. We will use the ratio of the scattering measured aboard the Cessna to the scattering measured aboard the Twin Otter as a first-order estimate of $FMF_{scat\_altitude}$, as shown in equation (1) below.

$$FMF_{scat\_altitude} \approx \frac{\sigma_{sp^{Cessna}}}{\sigma_{sp^{Twin\_Otter}}} \quad (1)$$

As discussed earlier, the Twin Otter inlet had a 50% cutoff at a particles diameter of approximately 8 μm. The CAPS in the wing-pod of the Twin Otter measured particle distribution (as shown later in Figure 7) with strong exponential decrease in particles sizes greater than 8 μm, suggesting that this definition of $FMF_{scat\_altitude}$ is a reasonable estimate.

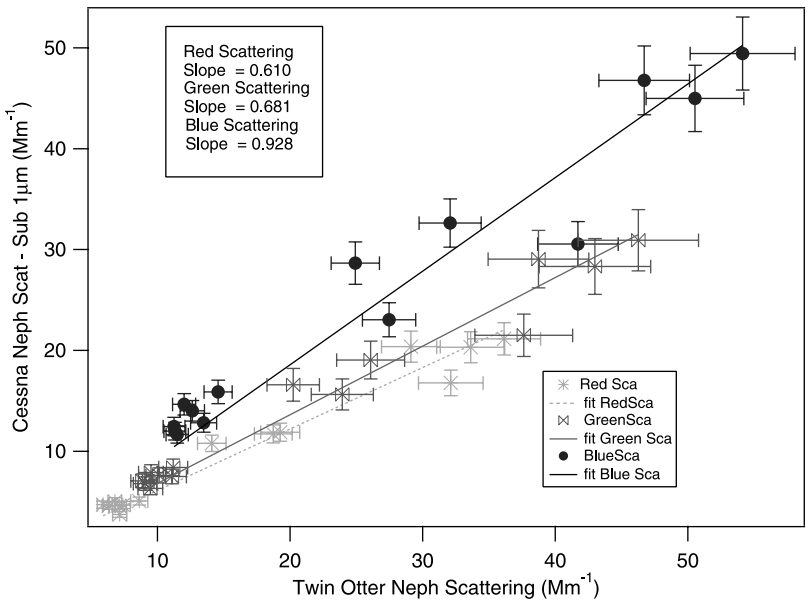

Figure 4. A comparison of the scattering coefficient measured by the TSI nephelometer aboard the IAP Cessna and the TSI nephelometer aboard the CIRPAS Twin Otter during simultaneous flight legs. These data points are representative of time periods in which both instruments measured with their standard inlet conditions (i.e., the Cessna was equipped with a 1 μm aerodynamic diameter impactor; the Twin Otter was equipped with inlet system, which has a 50% cutoff diameter at 8 μm). There is a significant decrease in the agreement between the two instruments as the wavelength increases. This trend is indicative of the sampling conditions (i.e., larger particles are being sampled in the Twin Otter nephelometer). Error bars represented reported 7.3%, 7.6%, and 9.8% uncertainty in TSI nephelometer blue, green, and red wavelengths, respectively [*Anderson et al.*, 1996].

[46] Overall, for the flight legs represented in Figure 4, there was a great deal of variability in the calculated $FMF_{scat\_altitude}$. For the red channel (675 nm), the ratio varied between 0.52 and 0.79, with a mean of 0.65. For the green channel (530 nm), the ratio varied between 0.57 and 0.83 with a mean of 0.72. Finally for the blue channel (467 nm), the ratio varied between 0.73 and 1.21, with a mean of 1.00.

[47] The ratio between the Cessna nephelometer and the Twin Otter nephelometer ($FMF_{scat\_altitude}$) were also plotted against altitude, for all three wavelengths. These plots were created to investigate the possibility of trends with altitude in supermicron particles. Distinct trends did not exist in the ratio between the two instruments at altitude, suggesting that the coarse mode is overall variable throughout the atmospheric column, as observed by *Andrews et al.* [2004]. Using the student T test for statistical significance of means, it should be noted that $FMF_{scat\_altitude}$ was also independent of flight and day.

[48] Additionally the contribution of scattering due to particles above 1 μm was calculated by taking the difference between scattering measured aboard the Twin Otter and the Cessna and dividing by the scattering measured aboard the Twin Otter. As expected on the basis of the $FMF_{scat\_altitude}$ information above, the contribution of scattering due to particles greater than 1 μm was highly variable aloft and did not correlate with altitude. For the red, green, and blue channels the contribution of particles aloft varied between 20–48%, 17–43%, and −21–26% respectively. The average value for the contribution of scattering due to particles above 1 μm for the red, green, and blue channels was 35%, 28%, and 1%. The blue channel comparison is again somewhat suspect, as will be shown in the next section.

[49] The $FMF_{scat\_altitude}$ calculated from these flight legs was compared to the TSI nephelometer located at the ACRF ground site. As mentioned in the introduction, the surface-based nephelometer system alternates between two size cuts, every 6 min, with a 1 μm and a 10 μm impactor, allowing for a calculation of fine mode fraction defined in equation (2).

$$FMF_{scat\_ground} = \frac{\sigma_{sp\_<1\,\mu m}}{\sigma_{sp\_<10\,\mu m}} \tag{2}$$

Table 2. Average Ratio of Measurements Between the Two Aircraft Nephelometers During Three Different Comparison Conditions

Cessna Nephelometer/Twin Otter Nephelometer	Blue 467 nm	Green 530 nm	Red 675 nm
All flights except 25 May	0.928	0.681	0.610
Flight only 25 May	1.297	0.973	0.925
Postmission ground-based comparison	0.917	0.896	0.807

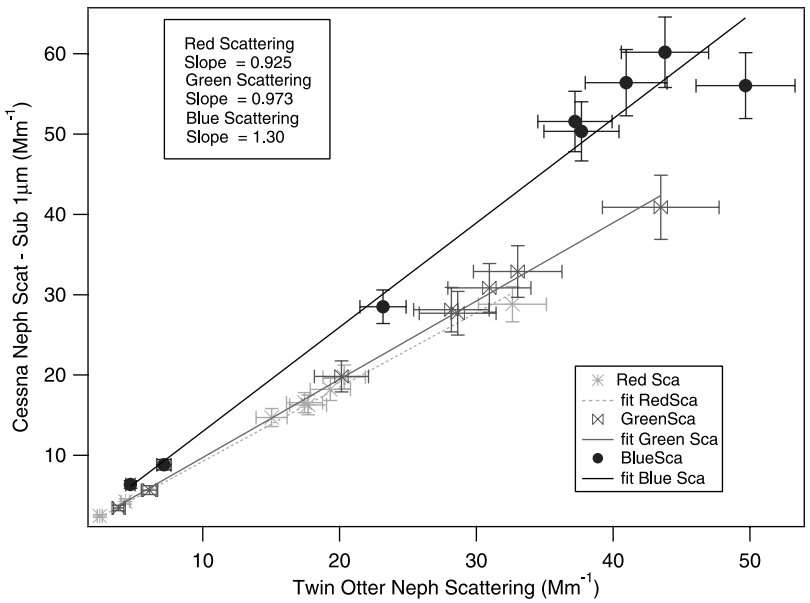

Figure 5. A comparison of the scattering coefficient measured by the TSI nephelometer aboard the IAP Cessna and the TSI nephelometer aboard the CIRPAS Twin Otter during simultaneous flight legs. These data points are representative of time periods in which both instruments measured with impactors (i.e., both the Cessna and Twin Otter nephelometers were equipped with a 1 μm aerodynamic diameter impactor). In comparison to Figure 4, there is better general agreement between the two instruments. The discrepancy between the two nephelometers at blue wavelength (467 nm) is surprising (see text for more details). Error bars represented reported 7.3%, 7.6%, and 9.8% uncertainty in TSI nephelometer blue, green, and red wavelengths, respectively [*Anderson et al.*, 1996].

During the flight legs, the ground-based FMF_{scat_ground} averaged 0.66, 0.80, and 0.73 for red, blue, and green channels respectively. There was no correlation seen between the ground-based FMF_{scat_ground} and the $FMF_{scat\_altitude}$ calculated from the Cessna and Twin Otter aloft. For example, on 7 May the average $FMF_{scat\_altitude}$ was plotted against the average FMF_{scat_ground} of the nearest corresponding time. The three corresponding r^2 values (corresponding to the red, blue, and green channels) of this comparison between the calculated ground and aloft FMF_{scat} were less than 0.01, emphasizing no correlation between these values.

[50] Next the two nephelometers were compared for only the flight legs on 25 May, in which both instruments sampled with a 1 μm impactor. This comparison is illustrated in Figure 5 and Table 2. This comparison includes 6 level legs. Again, these two instruments were well correlated with an r-squared value of 0.96 or greater. The ratio between measurements is close to unity for the green and red scattering measurements, as expected with both instruments (identical TSI nephelometers, same model number) measuring from a similarly restricted inlet system (i.e., attached to a 1 μm impactor). Yet surprisingly, the scattering measurements at the shortest wavelength (blue, 467 nm) show a large discrepancy between the instruments. The Cessna nephelometer measures about 30% higher than the Twin Otter nephelometer.

[51] Noting that we have already established the assumption that the two nephelometers were flying within the same aerosol sample (see section 3.1), the resulting figures (with a notable similar wavelength trends) lead to only two possible explanations: (1) There are systematic differences between these two essentially identical nephelometers (note: nephelometers are the same model from the same manufacturer). (2) The aircraft inlet systems affected the measurements, resulting in different particle sampling. These two possibilities will be addressed in the following sections. Section 4.3 discusses the possibility of systematic differences between the instruments. Finally, section 5 contains an extensive discussion of theoretical results pertaining to the aircraft inlet sampling conditions related to the size distributions measured aboard the Twin Otter.

4.3. Postmission Comparison Between the Cessna and Twin Otter Nephelometers

[52] A ground-based comparison of the TSI nephelometers deployed in the Aerosol IOP mission was performed at the end of the mission in the Greenwood Aviation hangar at Ponca City airport. The comparison included the nephelometer aboard the Cessna IAP aircraft, the nephelometer aboard the Twin Otter aircraft, and a ground-based nephelometer located at the SGP site during the Aerosol IOP mission. Again, all three instruments were TSI Model 3563 nephelometers.

[53] The instruments sampled from a common mixing chamber, which sampled ambient hangar aerosol. The aircraft instruments were disconnected from their inlets and impactors. Nearly equal lengths of conductive tubing directed aerosols into each nephelometer, thus the same types and amounts of particles should have made it into each instrument. The nephelometers were operated at the same ambient relative humidity, with only internal heating from lamp. During the comparison, the nephelometers

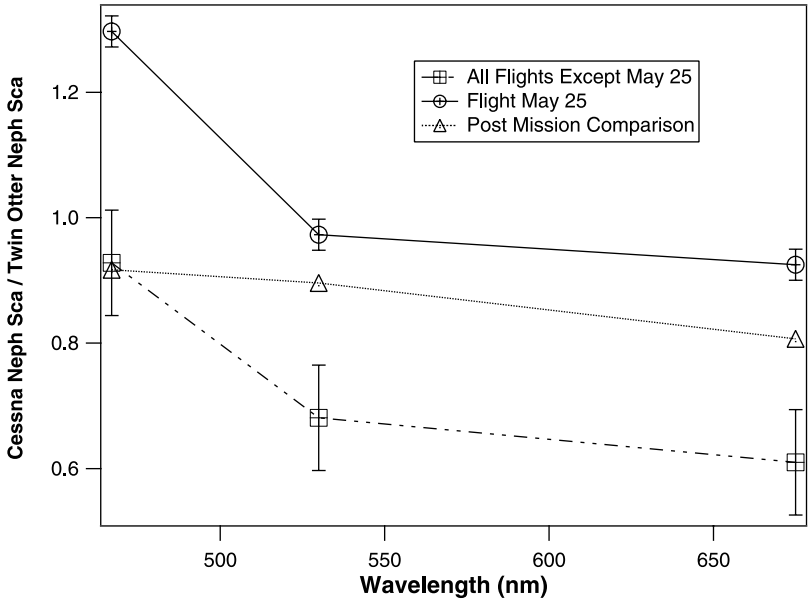

Figure 6. Ratio of scattering coefficient during the three comparison conditions as measured by the aircraft nephelometers. Squares represent instruments in flight, planes equipped with different inlet sampling systems. Circles represent instruments in flight, both planes equipped with 1 μm impactors. Triangles represent postmission ground-based comparison. See text for details.

measured scattering coefficients between 15 and 45 Mm^{-1}. Before the experiment the nephelometers were calibrated with CO_2 and filtered air. The results of these calibrations have not been incorporated into the calculations/results presented here. Thus this ground comparison should be representative of the instruments during the mission. The Cessna nephelometer and Twin Otter nephelometer were each compared directly to the ground-based nephelometer. The direct comparison between the two aircraft nephelometers was not done; instead a comparison was inferred with regard to the ground-based nephelometer. The results of this experiment/calculation are presented in Table 2 and Figure 6. The aircraft nephelometers agreed within 19% at all wavelengths.

[54] A summary of the results described in sections 4.2 and 4.3 is illustrated with Figure 6. Figure 6 represents data during the three comparison conditions between the aircraft nephelometers. The ratio of the Twin Otter and Cessna nephelometer scattering measurements is plotted for each wavelength. These ratios represent the mean value of all comparisons represented with the sample. The standard deviation from the mean for the aircraft measurements is represented in Figure 6 with the error bars. Plotted with square markers are the average results of conditions in which each aircraft had different inlets (all flight days except 25 May). Represented with circles are data only from 25 May (i.e., when both instruments had a 1 μm impactor). Finally, the postmission comparison is illustrated with triangles. The overall message of Figure 6 is that the strong wavelength dependence (found when comparing the aircraft nephelometers during flight) was not seen during the postmission ground-based comparison. Thus this postmission comparison provides clear evidence that the wavelength dependence seen within nephelometer comparison during flight cannot be attributed to systematic differences between the instruments.

5. Mie Scattering Calculations Using Size Distribution Data

[55] In order to investigate the possibility that different results from the two aircraft nephelometers were due to differences in the aircraft inlet systems, the aerosol size distributions were investigated. As described in section 2.4 and 2.5, there were two particle sizing probes aboard the Twin Otter, the PCASP and CAPS. Together these probes measure particles from 0.1–63 μm. A sample size distribution from a level leg flown on 9 May is shown in Figure 7. Overall, the size distributions measured by PCASP and CAPS show reasonable overlap, only considering the difference in sampling conditions between the two probes. Recall that the CAPS measured at ambient relative humidity, while the PCASP was heated. During this particular flight leg, the ambient relative humidity was low, varying between 30 and 45%.

[56] Using the known size range and bin width of the PCASP probes, the scattering efficiencies were calculated from Mie theory (using Wiscombe's code) [*Wiscombe*, 1980]. Because of the small number of size bins, the 20 bins were extrapolated to 100 points, for increased accuracy in the Mie calculations. This calculation was done for the three relevant wavelengths of 467 nm, 530 nm, and 675 nm at a range of complex indices of refraction between 1.53 ± 0.0007 and 1.43 ± 0.000000015. These indices of refraction were used on the basis of the work of *Clarke et al.* [2004] and the reported values of ''dust-like''/mineral material by *D'Almeida et al.* [1991] at 650 nm. These values also agree well with the range of real refractive indices derived by

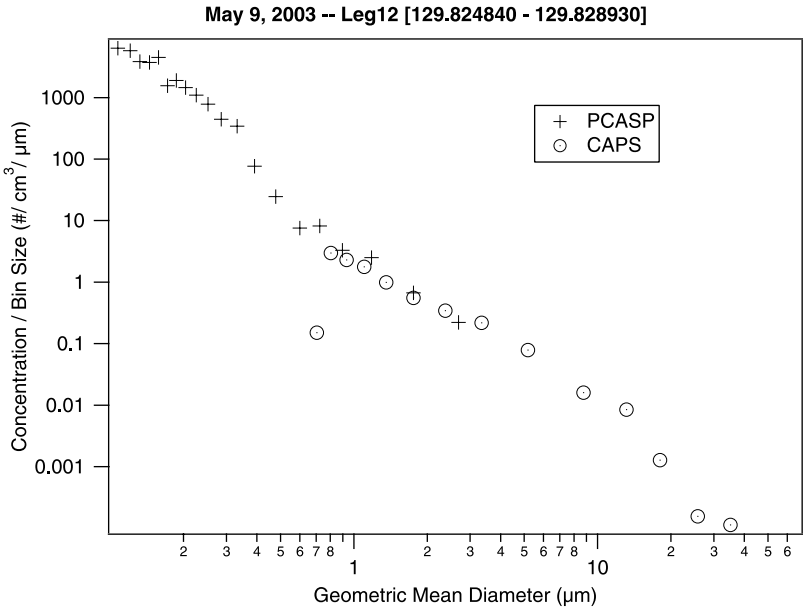

Figure 7. Typical size distribution from a level flight leg. The distribution includes both sizing probes aboard the Twin Otter, the PCASP and CAPS.

Ferrare et al. [2006] on the basis of measurements during the Aerosol IOP campaign. These scattering efficiencies were then combined with the measured size distributions for each level leg to calculate the scattering coefficients expected over the distribution using equation (3),

$$\sigma_{S_i} = \frac{\pi}{4} D_i^2 * Q_{S_i} * N_i \tag{3}$$

where σ_{si} is the scattering coefficient for the particles measured in the bin of index i, D_i is the geometric mean diameter of the particles measured within bin i, Q_{si} is the calculated Mie scattering efficiency for a particle of the size D_i, and N_i is the average number density measured by the probe with the size bin i.

[57] Illustrated in Figure 8 are the calculated coefficients (normalized to the bin size) for the size distributions measured by PCASP during a level leg (shown in Figure 7) flown on 9 May. Although there was a great deal of variation between the size distributions measured during each level leg, we feel that this particular leg is generally a representative case study of the mission. As shown in Figure 8, particle sizes greater than 0.79 μm (geometric diameter cut off point of the impactor aboard the Cessna aircraft) have a significant contribution to the scattering coefficient.

[58] Using the results presented in Figure 8a, the total scattering coefficient at 675 nm was calculated for each level leg by performing a summation across the distribution. To eliminate the uncertainty of combining the size distributions from the two separate probes (especially since the probes measured at different RH and f(RH) was not measured aloft), only the size distribution from the PCASP was considered. Consequently, the reported total extinction presented here represents only particles less than 3.1 μm. Figure 9 represents data from many of the level legs flown in formation between the Cessna and Twin Otter during Aerosol IOP. For each level leg, we calculated the relative contribution to the total calculated scattering coefficient at each size bin. In other words, the contribution of bins is accumulated as the size increases. In Figure 9, noted with the dark vertical line is the geometric size cut of the Cessna impactor (0.79 μm). This vertical line crosses the envelope of lines (leg 1 is the low value and leg 17 is the high value) representing cumulative scattering coefficients at range values of between 0.47 and 0.84. Thus during the level flight legs illustrated in Figure 9, theoretically the Cessna aircraft is measuring only between 47% and 84% of the scattering (at 675 nm and assuming a index of refraction of 1.53 ± 0.0007) with its current impactor. Using the method of *Wex et al.* [2002], discussed in more detail below, the uncertainty of the number size distribution measured with the PCASP was assumed to be ±½ channel. The dashed lines in Figure 9, represent ±½ channel at the pertinent size bin. The two dashed lines represent 0.65 μm and 1.16 μm. At the smaller limit (0.65 μm), theoretically the Cessna aircraft is measuring between 39% and 81% of the scattering with its current impactor. At the upper limit (1.16 μm), the Cessna is measuring between 67% and 91%.

[59] Next, the calculated scattering from the PCASP (at three wavelength of 467 nm, 530 nm, and 675 nm with an index of refraction of 1.53 ± 0.0007) was averaged over each level leg. This calculated average scattering coefficient was compared to the measured scattering coefficient from the Cessna nephelometer and agreed overall within approximately 40%; these two measurements were relatively well correlated ($r^2 \geq 0.88$). This comparison is illustrated in Figure 10 with shaded markers.

[60] Again using the results illustrated in Figure 8a (calculated PCASP scattering across the size distribution), the contribution of this scattering theoretically measured by the Cessna (with the impactor) was calculated. Instead of integrating across the entire size distribution (as shown in Figure 10 with the shaded markers), we integrated across

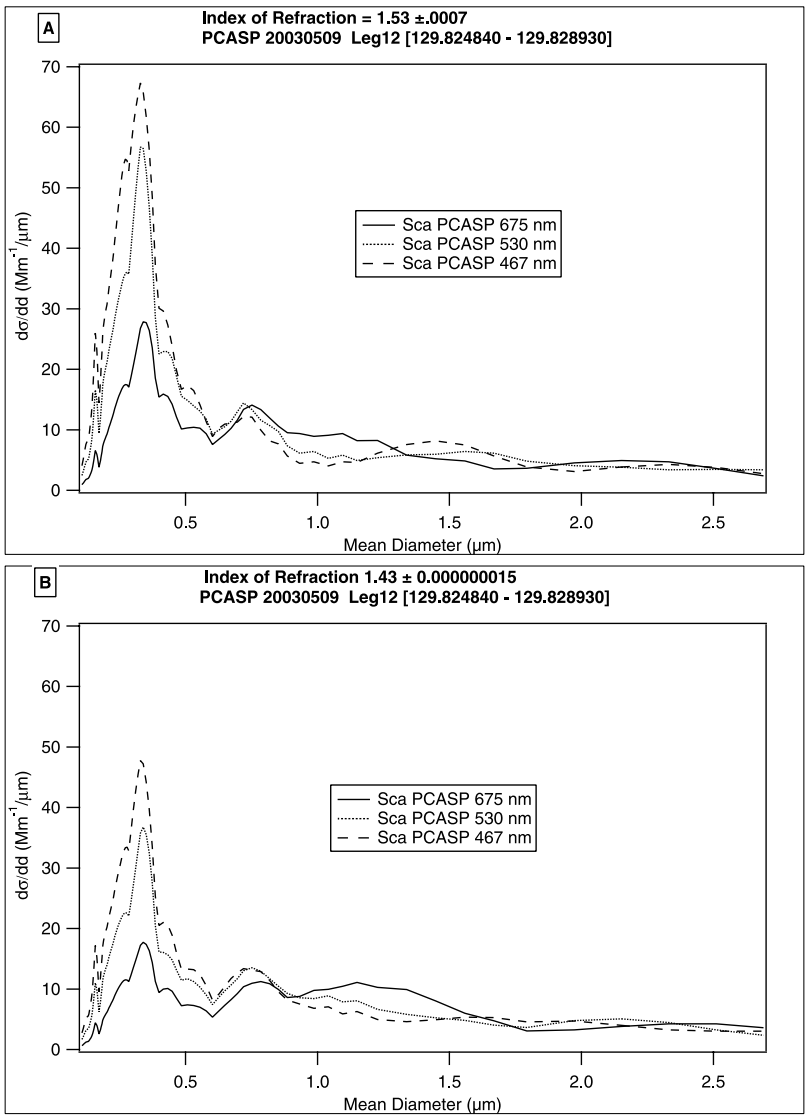

Figure 8. (a and b) Results of Mie scattering coefficients calculations across the size distribution using two indices of refraction with the size distribution shown in Figure 7 to calculate the scattering coefficient at three wavelengths (467, 530, and 675 nm). Note that there is a significant contribution to scattering particle size greater than the 0.79 μm, the geometric cutoff diameter of the Cessna impactor.

the size distribution only to the 1 μm size bin (i.e., the closest bin size to the 0.79 μm geometric cut off of the Cessna aircraft). The calculated average scattering from the PCASP data for particle sizes less than 1 μm is shown in Figure 10 with open symbols. As indicated by the slope of the line, the absolute agreement between the PCASP integrated to 1 μm and the measured nephelometer scattering is worse than the agreement between the total PCASP and the measured nephelometer scattering. Yet, the correlation between the PCASP integrated to 1 μm and the measured nephelometer scattering ($r^2 \geq 0.96$) is much better in this case.

[61] Finally, the calculated PCASP scattering was compared to the scattering measured aboard the Twin Otter with the nephelometer for each level flight leg. This comparison is shown in Figure 11 for the three measured wavelengths.

[62] The PCASP requires several assumptions to make measurement of size distributions, which lead to a greater uncertainty in the scattering coefficient calculated from PCASP data. The assumption included in the PCASP principle of operations is that scattered light is detected from a spherical particle with a refractive index of 1.58 (Note: Our Mie calculations illustrated in Figures 9 and 10 assume a refractive index of 1.53 + 0.0007i). Also as discussed in section 2.4, the relative humidity was not measured inside the PCASP. It is assumed that the relative humidity was close to zero, because of the extreme heating (20°C) created by the deicing heaters on the pod. The relative humidity within the nephelometers was approximately 30%, and thus the particles are assumed dry. It is acknowledge that extreme drying within the PCASP probe could have crystallized the aerosol and thus altered the shape. If the particles were initially spherical, the crystallization will increase the uncertainty within the Mie calculations, which assume spherical particles.

[63] The assumed difference in the relative humidity between the nephelometers and PCASP instruments may

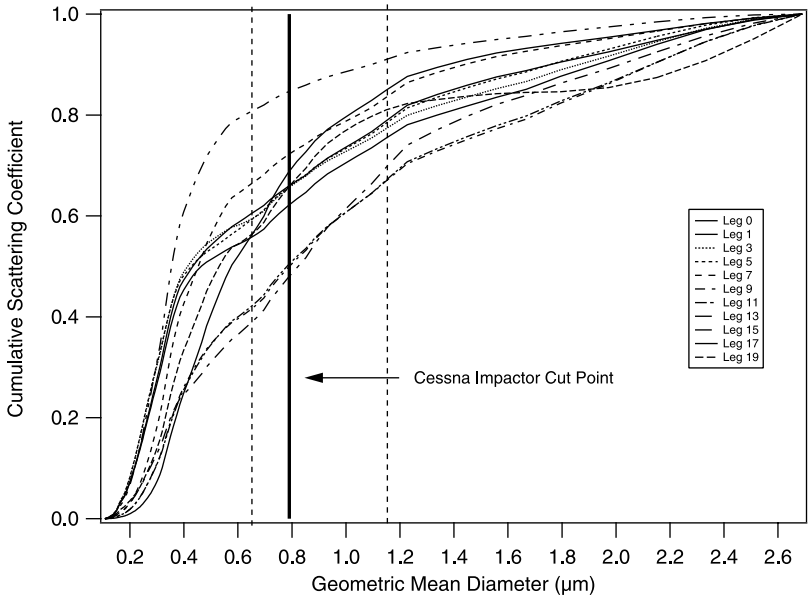

Figure 9. Cumulative scattering contribution (at 675 nm wavelength for an index of refraction of 1.53) across the size distribution. A significant sample of the level legs flown during Aerosol IOP is represented in the graph. For each level leg, the relative contribution to the total calculated scattering coefficient at each size bin was calculated. The dashed lines in Figure 9 represent ± ½ channel at the pertinent size bin (refer to text for further explanation).

explain the discrepancy between the measured Twin Otter nephelometer scattering and the calculated PCASP scattering. Overall, the total sensitivity of the Mie calculations on the uncertainty of the sizing with the PCASP must be examined. Using similar size distribution data, *Wex et al.* [2002] previously examined this uncertainty. The uncertainty of the number size distribution measured with the PCASP was assumed to be ±½ channel. The calculated scattering coefficient derived from the number size distributions, which were shifted toward the ±½ channel, differ from the original calculated scattering coefficient on the order of ±30%. Thus the uncertainty in the sizing has the dominate effect of the scattering coefficient.

[64] As in the previous figure, the absolute agreement between the measured scattering and that calculated from the PCASP is poor (slope $\leq$ 0.73). The fact that the correlation between the two measurements is excellent ($r^2 \geq 0.94$), as it was in Figure 10, provides strong evidence of the importance of this quantity in illustrating differences between the measurement techniques (i.e., different inlet systems) of the two aircraft. For the purposes of this study, the absolute value of the scattering coefficient calculated from the PCASP size distribution is not the main point, because it is acknowledged that there is a great deal of uncertainty associated with this calculation.

[65] With all these uncertainties in mind, it is likely that there is a systematic bias in the calculated scattering from the PCASP, eliminating the significance on the absolute value of the results. Thus more emphasis should be attributed to the correlation between the scattering coefficient calculated from the PCASP data and that measured with the Cessna nephelometer. The great improvement in the two correlations between the PCASP data and the Cessna nephelometer data (i.e., when the PCASP is integrated across the entire distribution compared to when the size distribution is only integrated to1 μm) is expected. This improved correlation highlights the effect of the 1 μm impactor on the Cessna nephelometer. Furthermore, the correlation is even better between the PCASP data and the Twin Otter nephelometer data (i.e., when the nephelometer and PCASP were measuring aboard the same plane).

6. Conclusion

[66] The long-term project, "In situ Aerosol Profiles (IAP) at SGP," which used a Cessna aircraft to measure aerosol optical properties in vertical profiles above the heavily instrumented SGP ground site, has been a success. This project has provided the first long-term (5 years) data set that characterizes the vertical distribution of aerosol optical properties. This long-term basis is necessary in order to adequately access the utility of ground-based in situ measurements for climate change research [*Andrews et al.*, 2004].

[67] As with any in situ data set, caution must be used when interpreting the results of the Cessna IAP measurements of optical properties. This paper presents a comparison of the Cessna IAP aircraft while in simultaneous flight paths with the CIRPAS Twin Otter aircraft during the May 2003 Aerosol IOP. Two instruments aboard the Twin Otter measured scattering coefficient at red wavelengths, a TSI nephelometer and Cadenza, which agreed very well, within 2%. Overall, it appears that the discrepancy between the similar TSI nephelometers' measurements of scattering coefficient, aboard the two different aircraft, was due to the aircraft sampling conditions. When the Twin Otter nephelometer was not attached to an impactor, the difference between the two nephelometers increased at longer

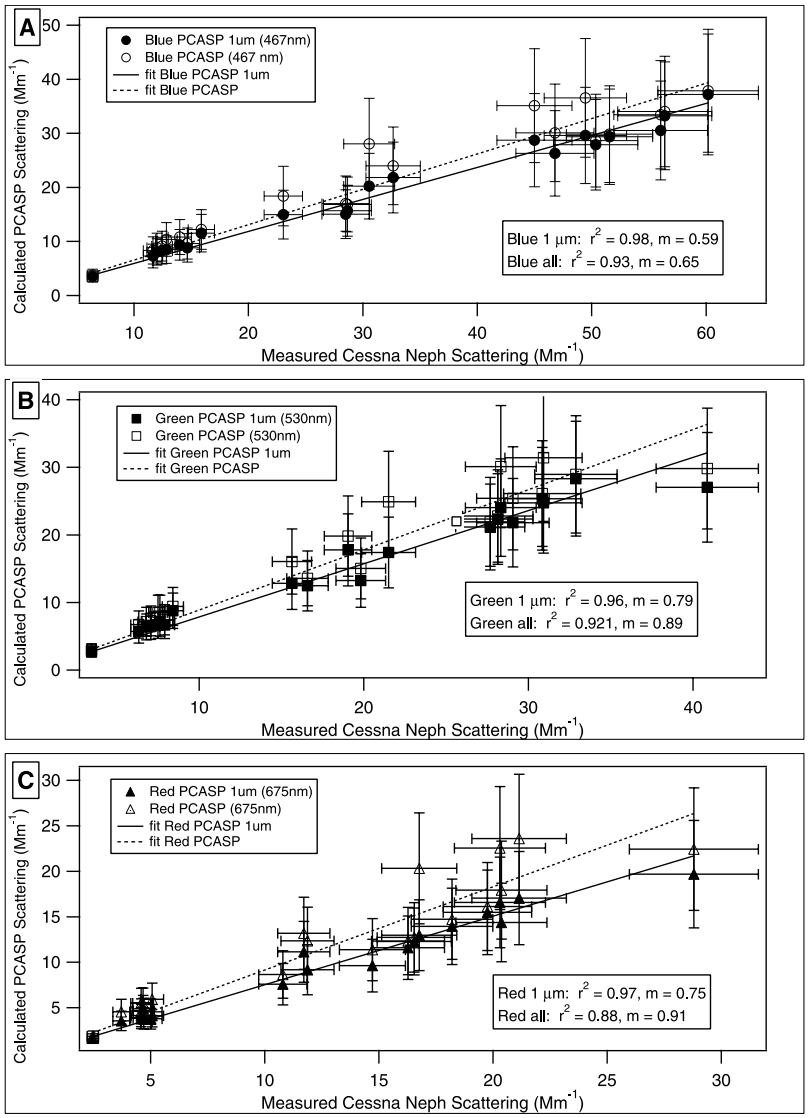

Figure 10. A comparison between the calculated scattering coefficient (at 467, 530, and 675 nm wavelengths using a real index of refraction of 1.53) and those measured with the TSI nephelometer on the Cessna aircraft. The calculated total scattering is represented by the open symbols, and the calculated scattering representing only particles sizes less than 1 μm is illustrated by the solid symbols. Although the absolute agreement between the two techniques is better in the case of total scattering, the correlation is better when considering only particles less than1 μm (see text for more details). Error bars represented reported 7.3%, 7.6%, and 9.8% uncertainty in TSI nephelometer blue, green, and red wavelengths, respectively. The 30% uncertainty in the calculated PCASP scattering is represented with error bars.

wavelengths; this behavior strongly suggests that the Cessna nephelometer was not sampling the large particles present due to the impactor. While both nephelometers were attached to an impactor (25 May), the agreement between the measurements improved in the red and green channels. Unexplained discrepancies between the two nephelometers aloft were observed in the blue channel. Additionally, this paper presents strong evidence in the form of theoretical Mie scattering calculations (using the measured size distributions) for the evidence of significant contribution of scattering from particles larger than the 1 μm cutoff diameter of the Cessna IAP aircraft.

[68] *Schmid et al.* [2006] looked at the results from six airborne field campaigns (all using different inlet conditions) conducted since 1996. In this study, airborne nephelometer measurements were added to PSAP measurements to obtain extinction coefficient, which was compared to the extinction coefficient of the NASA Ames Airborne Tracking 14-channel Sunphotometer (AATS-14). All instruments in this comparison were corrected to ambient conditions. Overall, the nephelometer plus PSAP measurements were consistently lower (<15% at visible wavelengths) when compared to airborne sunphotometer extinction data. Additionally, the discrepancy showed a strong wavelength dependence (i.e., the difference between the nephelometer plus PSAP/Cadenza and AATS-14 increased at longer wavelengths). *Strawa et al.* [2006] also demonstrate discrepancies between the calculated effective radius from

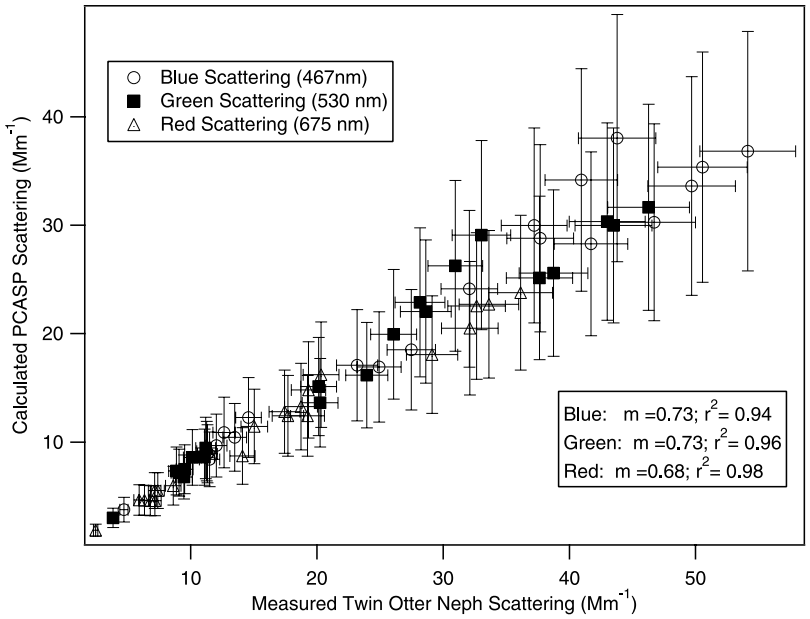

Figure 11. A comparison between the calculated scattering coefficient (at three wavelengths, 467 nm, 530 nm, and 675 nm, using a real index of refraction of 1.53) and the scattering coefficient measured with the TSI nephelometer aboard the Twin Otter aircraft. Error bars represented reported 7.3%, 7.6%, and 9.8% uncertainty in TSI nephelometer blue, green, and red wavelengths, respectively. Error bars represent a 30% uncertainty in the calculated PCASP scattering.

optical particle probes and other instrumentation aboard the Twin Otter during Aerosol IOP due to effects of inlet characterization. The results concluded above support the hypothesis that the inconsistency seen between remote measurements and nephelometers shown by *Schmid et al.* [2006] is likely due, at least in part, to particle sampling losses.

[69] Because of the variability in aerosol optical properties aloft, especially with respect to supermicron aerosols (as demonstrated in Figure 9 and section 4.2), applying ground-based corrections to the entire atmospheric column appears to be at best a first-order estimate. With this paper, we have highlighted the significant implications of particles larger than 1 μm aloft with respect to aerosol optical properties. This work strong supports the need for improved aircraft sampling techniques and in situ instrumentation for supermicron aerosol. Suggestions for inlet improvements include using well characterized diffuser inlets for all aerosol research aircraft. Currently ARM is building a diffuser inlet for the new Cessna 206 aircraft assigned to the ACRF site. Suggestions for an improved instrument for the measurement of coarse mode aerosol scattering include the development of an airborne integrating sphere nephelometer, which has very small truncation errors, with a fast response time [*Varma et al.*, 2003].

[70] **Acknowledgments.** This work was supported under the Atmospheric Radiation Measurement (ARM) program sponsored by the U.S. Department of Energy, Office of Science, Office of Biological and Environmental Research, Environmental Sciences Division. This work was also supported by NASA Upper Atmospheric Research and Radiation Science Programs. We thank the CIRPAS pilots and support team for their hard work during the field mission. This research was performed while the lead author (A.G. Hallar) held a National Research Council Research Associateship Award at NASA Ames Research Center. We also appreciate the helpful comments of the reviewers.

References

Anderson, T. L., and J. A. Ogren (1998), Determining aerosol radiative properties using the TSI 3563 intergrating nephelometer, *Aerosol Sci. Technol.*, *29*, 57–69.

Anderson, T. L., et al. (1996), Performance characteristics of a high-sensitivity, three-wavelength, total scatter/backscatter nephelometer, *J. Atmos. Oceanic Technol.*, *13*(5), 967–986.

Anderson, T. L., S. J. Masonis, D. S. Covert, N. C. Ahlquist, S. G. Howell, A. D. Clarke, and C. S. McNaughton (2003), Variability of aerosol optical properties derived from in situ aircraft measurements during ACE-Asia, *J. Geophys. Res.*, *108*(D23), 8647, doi:10.1029/2002JD003247.

Andrews, E., P. J. Sheridan, J. A. Ogren, and R. Ferrare (2004), In situ aerosol profiles over the Southern Great Plains cloud and radiation test bed site: 1. Aerosol optical properties, *J. Geophys. Res.*, *109*, D06208, doi:10.1029/2003JD004025.

Andrews, E., et al. (2006), Comparison of methods for deriving aerosol asymmetry parameter, *J. Geophys. Res.*, *111*, D05S04, doi:10.1029/2004JD005734.

Ångström, A. (1929), On the atmospheric transmission of Sun radiation and on dust in the air, *Geogr. Ann. Dtsch.*, *12*, 156–166.

Bane, J. M., R. Bluth, C. Flagg, H. Jonsson, W. K. Melville, M. Prince, and D. Riemer (2004), UNOLS now oversees research aircraft facilities for ocean science, *Eos Trans. AGU*, *85*(41), 402.

Baumgardner, D., H. Jonsson, W. Dawson, D. O'Connor, and R. Newton (2001), The cloud, aerosol and precipitation spectrometer: A new instrument for cloud investigations, *Atmos. Res.*, *59–60*, 251–264.

Blomquist, B. W., B. J. Huebert, S. G. Howell, M. R. Litchy, C. H. Twohy, A. Schanot, D. Baumgardner, B. Lafleur, R. Seebaugh, and M. L. Laucks (2001), An evaluation of the Community Aerosol Inlet for the NCAR C-130 research aircraft, *J. Atmos. Oceanic Technol.*, *18*, 1387–1397.

Busch, K. W., and M. A. Busch (1999), *Cavity Ringdown Spectroscopy*, Am. Chem. Soc., Washington, D. C.

Clarke, A. D., and R. J. Charlson (1985), Radiative properties of the background aerosol-absorption component of extinction, *Science*, *229*(4710), 263–265.

Clarke, A. D., W. G. Collins, P. J. Rasch, V. N. Kapustin, K. Moore, S. Howell, and H. E. Fuelberg (2001), Dust and pollution transport on global scales: Aerosol measurements and model predictions, *J. Geophys.Res.*, *106*, 32,555–32,569.

Clarke, A. D., et al. (2004), Size distributions and mixtures of dust and black carbon aerosol in Asian outflow: Physiochemistry and optical properties, *J. Geophys. Res.*, *109*, D15S09, doi:10.1029/2003JD004378.

Collins, D. R., et al. (2000), In situ aerosol-size distributions and clear-column radiative closure during ACE-2, *Tellus, Ser. B*, *52*(2), 498–525.

D'Almeida, G. A., P. Koepke, and E. P. Shettle (1991), *Atmospheric Aerosols—Global Climatology and Radiative Characteristics*, A. Deepak, Hampton, Va.

Damoah, R., N. Spichtinger, C. Forster, P. James, I. Mattis, U. Wandinger, S. Beirle, T. Wagner, and A. Stohl (2004), Around the world in 17 days—Hemispheric-scale transport of forest fire smoke from Russia in May 2003, *Atmos. Chem. Phys.*, *4*, 1311–1321.

Delle Monache, L., K. D. Perry, R. T. Cederwall, and J. A. Ogren (2004), In situ aerosol profiles over the Southern Great Plains coud and radiation test bed site: 2. Effects of mixing height on aerosol properties, *J. Geophys. Res.*, *109*, D06209, doi:10.1029/2003JD004024.

Doherty, S. J., P. K. Quinn, A. Jefferson, C. M. Carrico, T. L. Anderson, and D. Hegg (2005), A comparison and summary of aerosol optical properties as observed in situ from aircraft, ship, and land during ACE-Asia, *J. Geophys. Res.*, *110*, D04201, doi:10.1029/2004JD004964.

Ferrare, R., et al. (2006), Evaluation of daytime measurements of aerosols and water vapor made by an operational Raman lidar over the Southern Great Plains, *J. Geophys. Res.*, *111*, D05S08, doi:10.1029/2005JD005836.

Gao, S., D. A. Hegg, and H. Jonsson (2003), Aerosol chemistry, and light-scattering and hygroscopicity budgets during outflow from East Asia, *J. Atmos. Chem.*, *46*(1), 55–88.

Hansen, J., et al. (1998), Climate Forcing in the industrial age, *Proc. Natl. Acad. Sci. U. S. A.*, *95*, 12,753–12,758.

Hegg, D. A., D. S. Covert, H. Jonsson, and P. A. Covert (2005), Determination of the transmission efficiency of an aircraft aerosol inlet, *Atmos. Sci. Technol.*, *39*(10), 966–971.

Hermann, M., F. Stratmann, M. Wilck, and A. Wiedensohler (2001), Sampling characteristics of an aircraft-borne aerosol inlet system, *J. Atmos. Oceanic Technol.*, *18*, 7–19.

Houghton, J. T., et al. (2001), *Climate Change 2001: The Scientific Basis*, Cambridge Univ. Press, New York.

Huebert, B. J., G. Lee, and W. L. Warren (1990), Airborne aerosol inlet passing efficiency measurement, *J. Geophys. Res.*, *97*, 3815–3824.

Huebert, B. J., T. Bates, P. B. Russell, G. Shi, Y. J. Kim, K. Kawamura, G. Carmichael, and T. Nakajima (2003), An overview of ACE-Asia: Strategies for quantifying the relationships between Asian aerosols and their climatic impacts, *J. Geophys. Res.*, *108*(D23), 8633, doi:10.1029/2003JD003550.

Huebert, B. J., et al. (2004), Measureing the passing efficiency of an airborne low turbulence aerosol inlet, *Aerosol Sci. Technol.*, *38*, 803–826.

Jaffe, D., I. Bertschi, L. Jaeglé, P. Novelli, J. S. Reid, H. Tanimoto, R. Vingarzan, and D. L. Westphal (2004), Long-range transport of Siberian biomass burning emissions and impact on surface ozone in western North America, *Geophys. Res. Lett.*, *31*, L16106, doi:10.1029/2004GL020093.

Jonsson, H. H., et al. (1995), Performance of a focused cavity aerosol spectrometer for measurements in the stratosphere of particle size in the 0.06–2.0 μm diameter range, *J. Atmos. Oceanic Technol.*, *12*(1), 115–129.

Kramer, M., and A. Afchine (2004), Sampling characteristics of inlets operating at low U/U0 ratios: New insights from computational fluid dynamics (CFX) modeling, *J. Aerosol Sci.*, *35*, 683–694.

Krishnan, R., and V. Ramanathan (2002), Evidence of surface cooling from absorbing aerosols, *Geophys. Res. Lett.*, *29*(9), 1340, doi:10.1029/2002GL014687.

Lee, Y.-N., L. Bowerman, Z. Song, P. Sheridan, and J. Ogren (2003), Fine aerosol chemical composition at the ARM Southern Great Plains site during the 2003 Aerosol IOP, *Eos Trans. AGU*, *84*(16), Fall Meet. Suppl., Abstract A21E-1027.

McFarquhar, G. M., and A. J. Heymsfield (2001), Parameterizations of INDOEX microphysical measurements and calculations of cloud susceptibility: Applications for climate studies, *J. Geophys. Res.*, *106*, 28,675–28,698.

Mulholland, G. W., and N. P. Bryner (1994), Radiometric model of the transmission cell-reciprocal nephelometer, *Atmos. Environ.*, *28*(5), 873–887.

Murphy, D. M., and M. E. Schein (1998), Wind tunnel tests of a shrouded aircraft inlet, *Aerosol Sci. Technol.*, *28*, 33–39.

O'Keefe, A., and D. A. G. Deacon (1988), Cavity ring-down optical spectrometer for absorption measurements using pulsed laser sources, *Rev. Sci. Instrum.*, *59*(12), 2544–2551.

Romanini, D., A. A. Kachanov, N. S. Adeghi, and F. Stoeckel (1997), CW cavity ring down spectroscopy, *Chem. Phys. Lett.*, *264*(3–4), 316–322.

Schmid, B., et al. (2006), How well do state-of-the-art techniques measuring the vertical profile of tropospheric aerosol extinction compare?, *J. Geophys. Res.*, *111*, D05S07, doi:10.1029/2005JD005837.

Sheridan, P. J., et al. (2001), Four years of continuous surface aerosol measurements for the Department of Energy's Atmospheric Radiation Measurement Program Southern Great Plains Cloud and Radiation Testbed Site, *J. Geophys. Res.*, *106*(D18), 20,735–20,747.

Sheridan, P. J., et al. (2005), The Reno Aerosol Optics Study: An evaluation of aerosol measurement methods, *Aerosol Sci. Technol.*, *39*(1), 1–16.

Shinozuka, Y., et al. (2004), Sea-salt vertical profiles over the Southern and tropical Pacific oceans: Microphysics, optical properties, spatial variability, and variations with wind speed, *J. Geophys. Res.*, *109*, D24201, doi:10.1029/2004JD004975.

Smith, J. D., and D. B. Atkinson (2001), A portable pulsed cavity ring-down transmissometer for measurement of the optical extinction of the atmospheric aerosol, *Analyst*, *1126*, 1216–1220.

Stokes, G. M., and S. E. Schwartz (1994), The Atmospheric Radiation Measurement (ARM) Program: Programmatic background and design of the cloud and radiation testbed, *Bull. Am. Meteorol. Soc.*, *75*, 1201–1221.

Strawa, A. W., R. Castaneda, T. Owano, D. S. Baer, and B. A. Paldus (2003), The measurement of aerosol optical properties using continuous wave cavity ring-down techniques, *J. Atmos. Oceanic Technol.*, *20*, 454–465.

Strawa, A. W., et al. (2006), Comparison of in situ aerosol extinction and scattering coefficient measurements made during the Aerosol Intensive Operating Period, *J. Geophys. Res.*, *111*, D05S03, doi:10.1029/2005JD006056.

Tang, I. N., and H. R. Munkelwitz (1994), Water activities, densities, and refractive indices of aqueous sulfates and sodium nitrate droplets of atmospheric importance, *J. Geophys. Res.*, *99*, 18,801–18,808.

Varma, R., H. Moosmüller, and P. Arnott (2003), Toward and ideal integrating nephelometer, *Opt. Lett.*, *28*(12), 1007–1010.

Wang, J., et al. (2002), Clear-column radiative closure during ACE-Asia: Comparison of multiwavelength extinction derived from particle size and composition with results from Sun photometry, *J. Geophys. Res.*, *107*(D23), 4688, doi:10.1029/2002JD002465.

Wex, H., C. Neusüß, M. Wendisch, F. Stratmann, C. Koziar, A. Keil, A. Wiedensohler, and M. Ebert (2002), Particle scattering, backscattering, and absorption coefficients: An in situ closure and sensitivity study, *J. Geophys. Res.*, *107*(D21), 8122, doi:10.1029/2000JD000234.

Wiscombe, W. J. (1980), Improved Mie scattering algorithms, *Appl. Opt.*, *19*(9), 1505–1509.

E. Andrews, J. Ogren, and P. Sheridan, NOAA, Climate Monitoring and Diagnostics Laboratory, Boulder, CO 80305, USA.

K. Bokarius, A. G. Hallar, A. Luu, and A. W. Strawa, NASA Ames Research Center, Moffett Field, CA 94035, USA. (ahallar@mail.arc.nasa.gov)

D. Covert and R. Elleman, Department of Atmospheric Science, University of Washington, Seattle, WA 98195, USA.

R. Ferrare, NASA Langley Research Center, Hampton, VA 23681, USA.

H. Jonsson, Center for Interdisciplinary Remotely-Piloted Aircraft Studies, Marina, CA 93933, USA.

B. Schmid, Bay Area Environmental Research Institute, Sonoma, CA 95476, USA.